Article

Current Biology

Lung Mediated Auditory Contrast Enhancement Improves the Signal-to-Noise Ratio for Communication in Frogs

Graphical Abstract

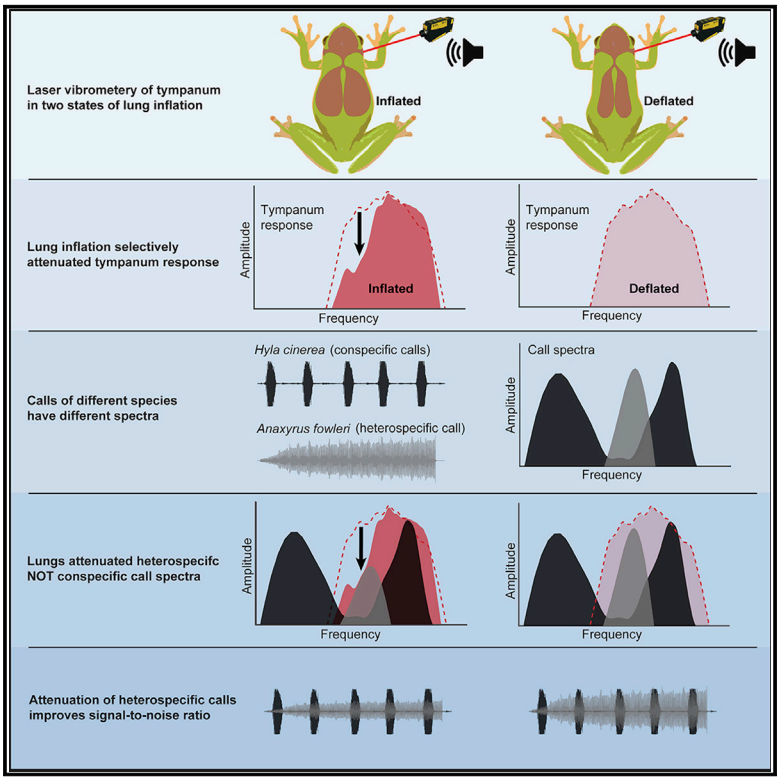

Highlights

- Lung resonance in frogs helps them solve a multi-species cocktail party problem
- Inflated lungs selectively attenuate eardrum vibrations at key sound frequencies
- Eardrums respond less to frequencies in other frog species' calls
- Sound transmission via the lungs enhances spectral contrast for noise control

Authors

Norman Lee, Jakob Christensen-Dalsgaard, Lauren A. White, Katrina M. Schrode, Mark A. Bee

Correspondence

lee33@stolaf.edu

In Brief

The noise characteristic of large social gatherings impairs effective vocal communication in humans and other animals. Lee et al. show that a lung-to-ear sound transmission pathway unique to amphibians helps frogs filter out noise to improve the signal-to-noise ratio for communication in noisy breeding choruses.

Lee et al., 2021, Current Biology *31*, 1–11
April 12, 2021
https://doi.org/10.1016/j.cub.2021.01.048

CellPress

Current Biology

CellPress
OPEN ACCESS

Article

Lung Mediated Auditory Contrast Enhancement Improves the Signal-to-Noise Ratio for Communication in Frogs

Norman Lee,[1,7,*] Jakob Christensen-Dalsgaard,[2] Lauren A. White,[3,6] Katrina M. Schrode,[4] and Mark A. Bee[3,4,5]
[1]Department of Biology, St. Olaf College, Northfield, MN 55057, USA
[2]Department of Biology, University of Southern Denmark, 5230 Odense M, Denmark
[3]Department of Ecology, Evolution, and Behavior, University of Minnesota - Twin Cities, St. Paul, MN 55108, USA
[4]Graduate Program in Neuroscience, University of Minnesota - Twin Cities, Minneapolis, MN 55455, USA
[5]Senior author
[6]Present address: USAID Office of HIV/AIDS, Washington, D.C., 20004
[7]Lead contact
*Correspondence: lee33@stolaf.edu
https://doi.org/10.1016/j.cub.2021.01.048

SUMMARY

Environmental noise is a major source of selection on animal sensory and communication systems. The acoustic signals of other animals represent particularly potent sources of noise for chorusing insects, frogs, and birds, which contend with a multi-species analog of the human "cocktail party problem" (i.e., our difficulty following speech in crowds). However, current knowledge of the diverse adaptations that function to solve noise problems in nonhuman animals remains limited. Here, we show that a lung-to-ear sound transmission pathway in frogs serves a heretofore unknown noise-control function in vertebrate hearing and sound communication. Inflated lungs improve the signal-to-noise ratio for communication by enhancing the spectral contrast in received vocalizations in ways analogous to signal processing algorithms used in hearing aids and cochlear implants. Laser vibrometry revealed that the resonance of inflated lungs selectively reduces the tympanum's sensitivity to frequencies between the two spectral peaks present in conspecific mating calls. Social network analysis of continent-scale citizen science data on frog calling behavior revealed that the calls of other frog species in multi-species choruses can be a prominent source of environmental noise attenuated by the lungs. Physiological modeling of peripheral frequency tuning indicated that inflated lungs could reduce both auditory masking and suppression of neural responses to mating calls by environmental noise. Together, these data suggest an ancient adaptation for detecting sound via the lungs has been evolutionarily co-opted to create auditory contrast enhancement that contributes to solving a multi-species cocktail party problem.

INTRODUCTION

Noise fundamentally impacts the function and evolution of diverse biological systems,[1,2] from cellular signaling pathways[3,4] and gene expression[5,6] to neural coding[7,8] and communication between whole organisms.[9–11] In the context of animal behavior, noise introduces errors in processing biologically relevant communication signals tightly linked to evolutionary fitness.[12–14] These errors manifest as higher signal detection thresholds,[15] poorer source localization,[16] impaired sound pattern recognition,[17] and reduced auditory discrimination.[18] There is widespread and increasing interest in understanding how animals are adapted to cope with noise problems,[9–11] particularly in light of increasing anthropogenic noise pollution.[19,20] For many insects,[21] frogs,[22] and birds[23] that signal acoustically in large and often multi-species aggregations, the signals of other individuals represent particularly potent sources of noise that reduce the signal-to-noise ratio for communication.[24] In essence, these animals must solve multi-species analogs of the human "cocktail party problem," which refers to our difficulty understanding speech in a noisy crowd.[25,26] Discovering how animals are adapted to cope with noise is key to understanding the mechanisms and evolution of their sensory and communication systems and assessing threats posed by anthropogenic noise. At present, however, knowledge of the diversity of these adaptations remains limited.

Frogs represent important taxa for uncovering independently evolved solutions to noise problems.[22,27,28] Among terrestrial vertebrates, there were multiple origins of tympanic middle ears during the Triassic period, one of which occurred in the lineage leading to modern frogs.[29] In addition, vocal communication evolved independently in frogs some 200 million years ago (probably after the origin of tympanic middle ears)[30] and is fundamental to reproduction in most extant frogs. Male frogs aggregate in dense breeding choruses, often comprising hundreds of individuals of multiple species, where they produce

Please cite this article in press as: Lee et al., Lung Mediated Auditory Contrast Enhancement Improves the Signal-to-Noise Ratio for Communication in Frogs, Current Biology (2021), https://doi.org/10.1016/j.cub.2021.01.048

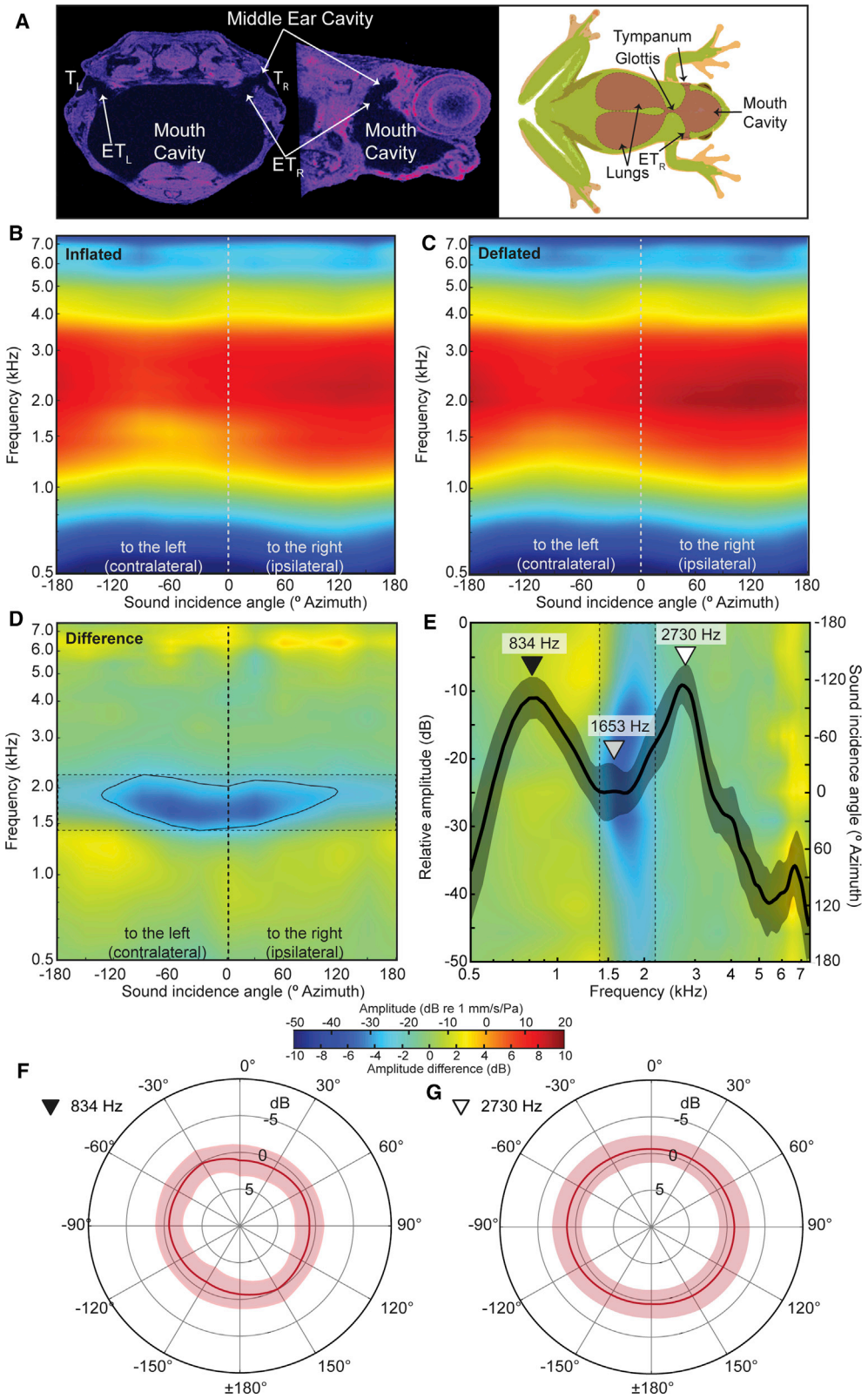

(legend on next page)

Please cite this article in press as: Lee et al., Lung Mediated Auditory Contrast Enhancement Improves the Signal-to-Noise Ratio for Communication in Frogs, Current Biology (2021), https://doi.org/10.1016/j.cub.2021.01.048

sexual signals (advertisement calls) to attract mates and repel rivals.[22,27,28] Advertisement calls are the most frequent vocalization produced by frogs, and they are produced at high sound amplitudes, with peak sound pressure levels (SPL) commonly exceeding 100 dB (at 1 m).[31] Consequently, frog breeding choruses can be characterized by high and sustained levels of noise.[32,33] Background noise and the overlapping calls of conspecific and heterospecific males within a chorus are potent sources of selection on frog communication given their ability to negatively impair auditory perception and degrade the mating decisions of females.[22,34]

Among extant terrestrial vertebrates, frogs and other amphibians are unique in having a lung-to-ear sound transmission pathway.[35–39] The tympanic middle ears of frogs are internally coupled through the mouth cavity via wide and open Eustachian tubes. Sound also reaches the internal surface of each tympanum through the body wall and air-filled lungs via the glottis, mouth, and Eustachian tubes (Figure 1A).[35–41] There is a potentially strong coupling between the frog's air-filled tympanic middle ears and its lungs, which remain inflated for relatively long periods punctuated by brief episodes of ventilation, and which remain continuously pressurized above atmospheric pressure during the respiratory cycle.[38,42] Thus, the response of each tympanum reflects the summation of sound impinging directly on its external surface and indirectly on its internal surface via input through the lungs and the opposite, internally coupled tympanum.[40] The function of the frog's lung-to-ear sound transmission pathway in hearing and vocal communication has remained elusive ever since its initial discovery.[35,40,41,43]

Because the frog's lungs are large air-filled cavities overlain by a relatively thin body wall, they resonate in response to sound.[35,39] Resonators feature prominently in musical instrument design,[44] engineering noise control,[45] and biological systems[46] because they can be specified to either amplify or attenuate certain sound frequencies. Here, we tested the hypothesis that the resonance of the frog's lungs and lung-to-ear sound transmission function to improve the signal-to-noise ratio for vocal communication by creating *spectral contrast enhancement* (SCE). Spectral contrast refers to the difference in amplitude (in dB) between the "peaks" and "valleys" in a sound spectrum. In the context of human hearing and speech communication, digital signal processing algorithms for SCE can either amplify the formant frequencies (peaks) of voiced speech sounds or attenuate frequencies between adjacent formants (valleys) in real time.[47–49] The SCE hypothesis predicts that lung-to-ear sound transmission either selectively amplifies the tympanum's response (i.e., increases its sensitivity) to frequencies in conspecific advertisement calls or selectively attenuates the tympanum's response (i.e., decreases its sensitivity) to non-call frequencies that may be characteristic of environmental noise, or both. These predictions were tested using females of the American green treefrog (*Hyla cinerea*; Hylidae). In this species, males call to attract females in noisy breeding choruses, often with multiple other frog species, and females choose their mate based on perceived features of his calls.[27] Using laser vibrometry and a model of tympanic responses, we show that the state of lung inflation has no impact on the tympanum's sensitivity to the species' own calls, but that inflated lungs resonate and selectively attenuate tympanum vibrations in a restricted but biologically important frequency range. By combining bioacoustic analyses of recorded calls with social network analyses of long-term citizen science data, we show that inflated lungs attenuate the tympanum's response to frequencies present in the calls of other frog species commonly encountered in multispecies choruses. A physiological model of sound processing by the peripheral auditory system suggests the acoustic benefits of inflated lungs are realized in reduced energetic masking and reduced suppression of neural responses to conspecific calls.

RESULTS

Inflated lungs selectively attenuate tympanum vibrations to non-call frequencies

We measured the tympanum's vibration amplitude while the lungs were in a naturally inflated state and after manual deflation of the lungs. In response to a frequency modulated (FM) sweep (175 ms, 0.2 to 7.5 kHz) broadcast from each of 12 equally spaced locations surrounding the animal (n = 21; Figure S1A), the tympanum responded to a broad range of frequencies between ~700 and ~7000 Hz, with maximum vibration amplitudes occurring in response to sounds coming from an ipsilateral direction (Figures 1B and 1C).[43] Differences in the tympanum's sensitivity between the inflated and deflated states were most pronounced between 1400 and 2200 Hz, where tympanum vibration amplitude was attenuated in the inflated state (Figure 1D).

Figure 1. Inflated lungs selectively attenuate tympanum vibrations to non-call frequencies

(A) Left: Magnetic resonance images (coronal, left; sagittal, right) of a green treefrog head showing the internal coupling of the left (L) and right (R) tympana (T) and air-filled middle ear cavities through the Eustachian tubes (ET) and mouth cavity. Right: Illustration showing the coupling of the lungs through the glottis to the internally coupled tympana and mouth cavity.

(B and C) Heatmaps showing the mean vibration amplitudes of the right tympanum in response to free-field acoustic stimulation in the inflated (B) and deflated (C) states of lung inflation across frequency and sound incidence angle (n = 21 individuals).

(D) Heatmap showing the mean differences between the vibration amplitudes of the tympanum in the inflated and deflated states of lung inflation (inflated – deflated) across frequency and sound incidence angle (n = 21 individuals). The black contour encloses frequencies and angles where attenuation of the tympanum's response equaled or exceeded −4 dB (i.e., values ≤ -4 dB) when the lungs were inflated compared with deflated. The minimum and maximum frequencies enclosed by the contour are 1400 and 2200 Hz, respectively. The dashed lines and shaded box enclose frequencies between 1400 and 2200 Hz across all angles.

(E) Frequency spectrum of the green treefrog advertisement call overlaid on a heatmap showing lung-mediated effects on tympanic sensitivity (redrawn from Figure 1D and rotated 90° clockwise). The thick black line and shaded gray area depict the mean ± 1 SD call spectrum (n = 23 males, 457 individual calls). The dashed lines and shaded box enclose frequencies between 1400 and 2200 Hz across all angles.

(F and G) Polar plots showing the mean ± 95% CI difference (in dB) in the tympanum's response between the inflated and deflated conditions (inflated – deflated) at the frequencies of the two spectral components of conspecific calls.

Please cite this article in press as: Lee et al., Lung Mediated Auditory Contrast Enhancement Improves the Signal-to-Noise Ratio for Communication in Frogs, Current Biology (2021), https://doi.org/10.1016/j.cub.2021.01.048

The prediction that inflated lungs could amplify the tympanum's response to frequencies emphasized in conspecific calls was not supported. Similar to other frogs in the genus *Hyla*,[27] male green treefrogs produce advertisement calls with two prominent spectral peaks that are analogous to the formant frequencies of human vowel sounds.[50] In a sample of 457 advertisement calls (~20 calls from each of 23 males), the mean (±SD) frequencies of the two peaks were 834 ± 14 Hz and 2730 ± 34 Hz (Figure 1E). Across angles of sound incidence, the mean (±95 CI) magnitude of the tympanum's vibration amplitude at 834 Hz and 2730 Hz differed between the inflated and deflated lung states by just 0.7 ± 1.8 dB (Figure 1F) and 0.8 ± 1.8 dB (Figure 1G), respectively; these mean values were not significantly different from zero (two-tailed, one-sample t tests: $t_{20} = 0.8$ and $t_{20} = 0.9$, respectively, ps > 0.393). Increases in vibration amplitude at other (i.e., non-call) frequencies were uniformly small (e.g., < ~3 dB) and either occurred when sounds were presented from behind the animal (e.g., −90° to −180°; Figure 1D) or at high frequencies (e.g., > 6000 Hz; Figure 1D) at which neither the tympanum (*cf.* Figures 1B and 1C) nor the peripheral auditory nervous system[51,52] is very sensitive.

Compared with the deflated state, inflated lungs selectively attenuated the tympanum's vibration amplitude in response to non-call frequencies in the range of 1400 to 2200 Hz (Figure 1D). Within this frequency range, the maximum attenuation of tympanum vibration amplitude, averaged across individuals (mean ± 95% CI), was −10.0 ± 1.8 dB (range: −3.3 to −17.4 dB) and was significantly different from zero (two-tailed, one-sample t test: $t_{20} = 10.91$, $p < 0.001$). Across individuals, the maximum attenuation occurred at a mean (±SD) frequency of 1726 ± 268 Hz. Mean values of attenuation on the order of −4 to −6 dB were common across frequencies between 1400 and 2200 Hz (Figure 1D), a range that fell precisely between the two spectral peaks of the advertisement call and encompassed the prominent spectral valley between them (Figure 1E). This spectral valley had a mean (±SD) center frequency of 1653 ± 39 Hz (Figure 1E). Attenuated vibration amplitudes spanned the frontal hemifield, but the bandwidth and magnitude of attenuation were somewhat larger when sound originated from within the contralateral portion of the frontal hemifield (i.e., between 0° and −90°; Figure 1D). Across individuals, the modal and median sound incidence angles corresponding to the maximum attenuation in tympanum vibration amplitude were −60° and −30°, respectively.

Together, these findings are consistent with the SCE hypothesis, according to which spectral contrast is enhanced by attenuating frequencies between the spectral peaks in vocalizations. Lung inflation had no impact on tympanic sensitivity to conspecific calls. Rather, inflated lungs created a "notch filter" that reduced tympanic sensitivity in a select range of sound frequencies (1400 to 2200 Hz) between the spectral peaks of the call. To further characterize this pulmonary notch filter, we used laser vibrometry to measure the resonance of lungs insonified by the same FM sweep (Figure S1B). These measurements confirmed that inflated lungs exhibit a prominent resonance that overlaps with the frequency range in which they also attenuate the tympanum's response. The mean (±95% CI) peak resonance frequency was 1558 ± 89 Hz (range: 1400 Hz to 1850 Hz; n = 10), and the mean (±95% CI) frequencies 10 dB down from the peak were 1244 ± 76 Hz and 1906 ± 151 Hz (Figures 2A and S2). There was a significant negative correlation between peak resonance frequency and body size, as expected if lung volume varies directly with body size (Figure S2; two-tailed Pearson $r = -0.705$, $R^2 = 0.498$, $p = 0.0228$). Manually deflating the lungs significantly attenuated the magnitude of the peak resonance frequency by −57.6 ± 6.0 dB (Figure 2A; two-tailed, one-sample t test: $t_9 = 18.7$, $p < 0.0001$). Following manual reinflation of the lungs, the mean (±95% CI) peak frequency of the lung resonance was restored (1627 ± 98 Hz; range: 1450 Hz to 1928 Hz) and did not differ from that measured in the original inflated state (Figure 2A; two-tailed, paired t test: $t_9 = 1.88$, $p = 0.0922$).

We further investigated the effects of the lung resonance by modeling how sound transmission via inflated and insonified lungs impacts the tympanum's response to free-field sound. The model compared reconstructions of the tympanum's free-field vibration amplitude in the inflated versus deflated states to determine the magnitudes of sound inputs to the two sides of the tympanum. The tympanum's response across frequency and azimuth was reconstructed by combining the magnitude of direct sound input arriving at its external surface with the transmission of indirect sound arriving at its internal surface via the contralateral tympanum and lungs, which we measured separately using local acoustic stimulation and laser vibrometry (n = 6; Figures S1C and S3). Across reconstructions, we varied the weighting of the measured lung transmission gain from 0 × to 6 × (see Methods and Figure S3 legend). A weighting of 0 × corresponds to the deflated state, and positive weightings correspond to the inflated state. We explored a range of positive weightings because local acoustic stimulation of the body wall (Figure S1C) potentially underestimates the real magnitude of lung-to-ear sound transmission due to the much larger surface area of the body wall exposed to sound during free-field acoustic stimulation. The model computed the difference between the 0 × weighting (deflated) and each positive weighting (inflated), such that the model's output reflects the expected impact of sound transmission via the lungs on the tympanum's vibration amplitude.

The model confirmed a predominant subtractive effect of the lung input on the magnitude of the tympanum's response to free-field sound (Figure 2B). The median peak transmission gain for the lung input under local acoustic stimulation occurred at 1430 Hz (Figure S3), which falls within the range of the lung's peak resonance frequencies measured with free-field acoustic stimulation (1400 Hz to 1850 Hz; Figures 2A). Relative to the deflated state (0 ×), tympanum responses reconstructed for the inflated state were attenuated between 1400 and 2200 Hz at all positive weightings of lung-to-ear sound transmission tested (1 × to 6 × ; Figure 2B). At a weighting of 4 × , inflated lungs attenuated tympanum vibration amplitude in this frequency range by approximately −4 to −6 dB, on average, at −60° azimuth. This attenuation is similar in magnitude to that observed when the tympanum's responses were measured directly under free-field conditions (*cf.* Figures 1D and 2B). Across additional angles of sound incidence, the model's output showed broad patterns consistent with those measured directly under free-field conditions: tympanum vibrations were attenuated within the frequency range of 1400 to 2200 Hz when the lungs were inflated, and attenuation was most pronounced at contralateral angles (*cf.* Figures 1D and 2C).

Please cite this article in press as: Lee et al., Lung Mediated Auditory Contrast Enhancement Improves the Signal-to-Noise Ratio for Communication in Frogs, Current Biology (2021), https://doi.org/10.1016/j.cub.2021.01.048

CellPress
OPEN ACCESS

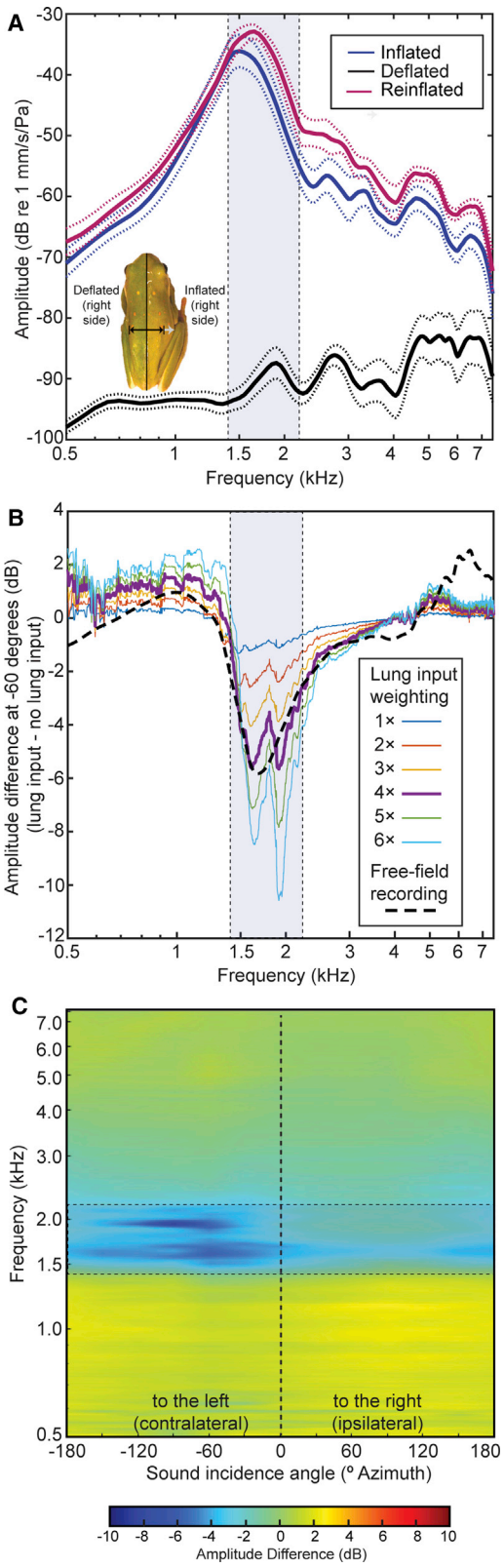

Figure 2. Lung resonance generates a tympanic notch filter

(A) Mean (solid lines; n = 10 individuals) ± 95% CIs (dashed curves) vibration amplitudes of the body wall above the right lung in the inflated, deflated, and reinflated conditions (Figure S2). *Inset:* A split image of a female green treefrog showing the lateral extension of her right body wall in the inflated (non-reflected right half of image) and deflated (reflected left half of image) states of lung inflation. Black arrows depict the lateral extension of the female's right body wall in the deflated state, and the light gray arrow depicts the additional lateral extension of the right body wall in the inflated condition.

(B) The modeled impact of inflated lungs on the magnitude of difference between reconstructed free-field responses of the tympanum to sound from a contralateral angle of −60° in the inflated and deflated states (Figure S3). Model output is shown for six transmission gain weightings (1 × to 6 ×) of the lung input relative to no lung input (0 ×). The actual impacts of the lung on the tympanum's free-field response are shown by the dashed black line (redrawn from the −60° contour in the heatmap in Figure 1D), which closely matches the predicted response for a lung transmission gain weighting of 4 × .

(C) Model output for the predicted effects of inflated lungs on the tympanum's free-field response across frequency and sound incidence angle using a lung input weighting of 4 × .

In all panels (A–C), the dashed lines and shaded blue rectangle enclose frequencies between 1400 Hz and 2200 Hz.

Inflated lungs attenuate tympanum vibrations to heterospecific calls

The calls of other frog species in multi-species breeding choruses represent prominent sources of environmental noise that interfere with communication.[22,27,28] Therefore, we evaluated the extent to which the calls of heterospecific frogs breeding at the same times and places as green treefrogs constitute environmental noise in the frequency range attenuated by the lungs. To this end, we integrated analyses of continent-scale citizen science data from the North American Amphibian Monitoring Program (NAAMP)[53,54] with bioacoustic analyses of archived recordings of frog calls. NAAMP was a long-term (1994-2015) effort to monitor frog populations using roadside calling surveys conducted across 26 states that encompass most of the green treefrog geographic range in the eastern, central, and southern United States. In the NAAMP dataset, there were 19,809 reports of "co-calling" between green treefrogs and a total of 42 other species, meaning these 42 species were observed calling at the same times and places as our focal species (Figure S4).

Social network analysis revealed that just 10 of the 42 co-calling heterospecific species (i.e., 24% of all co-calling species) accounted for the overwhelming majority (79%) of the observed instances of co-calling between green treefrogs and one or more other species in the NAAMP dataset (Figures 3 and S4). Of these top-10 heterospecific species, half (i.e., 5 of 42 total heterospecific species, or 12%) accounted for 42% of all instances of co-calling and produce advertisement calls with prominent spectral peaks falling in the range of 1400 to 2200 Hz (Figure 3). One of these five species, for example, is Fowler's toad (*Anaxyrus fowleri*), which produces a long, loud call with a single spectral peak in the range of 1400 to 2200 Hz (Figure 3). Others of these five species, such as the North American bullfrog (*Lithobates catesbeianus*), the green frog (*Lithobates clamitans*), and the barking treefrog (*Hyla gratiosa*) produce calls with bimodal spectra in which one of two spectral components falls within the range of 1400 to 2200 Hz (Figure 3). We selected these five heterospecific species to model the impacts of lung mediated notch filtering on the tympanum's response to heterospecific calls. The average spectra of their advertisement calls were passed through simulated tympanic filters corresponding to 0° (frontal) and −30° and −60° (contralateral) with the lungs inflated versus deflated.

Please cite this article in press as: Lee et al., Lung Mediated Auditory Contrast Enhancement Improves the Signal-to-Noise Ratio for Communication in Frogs, Current Biology (2021), https://doi.org/10.1016/j.cub.2021.01.048

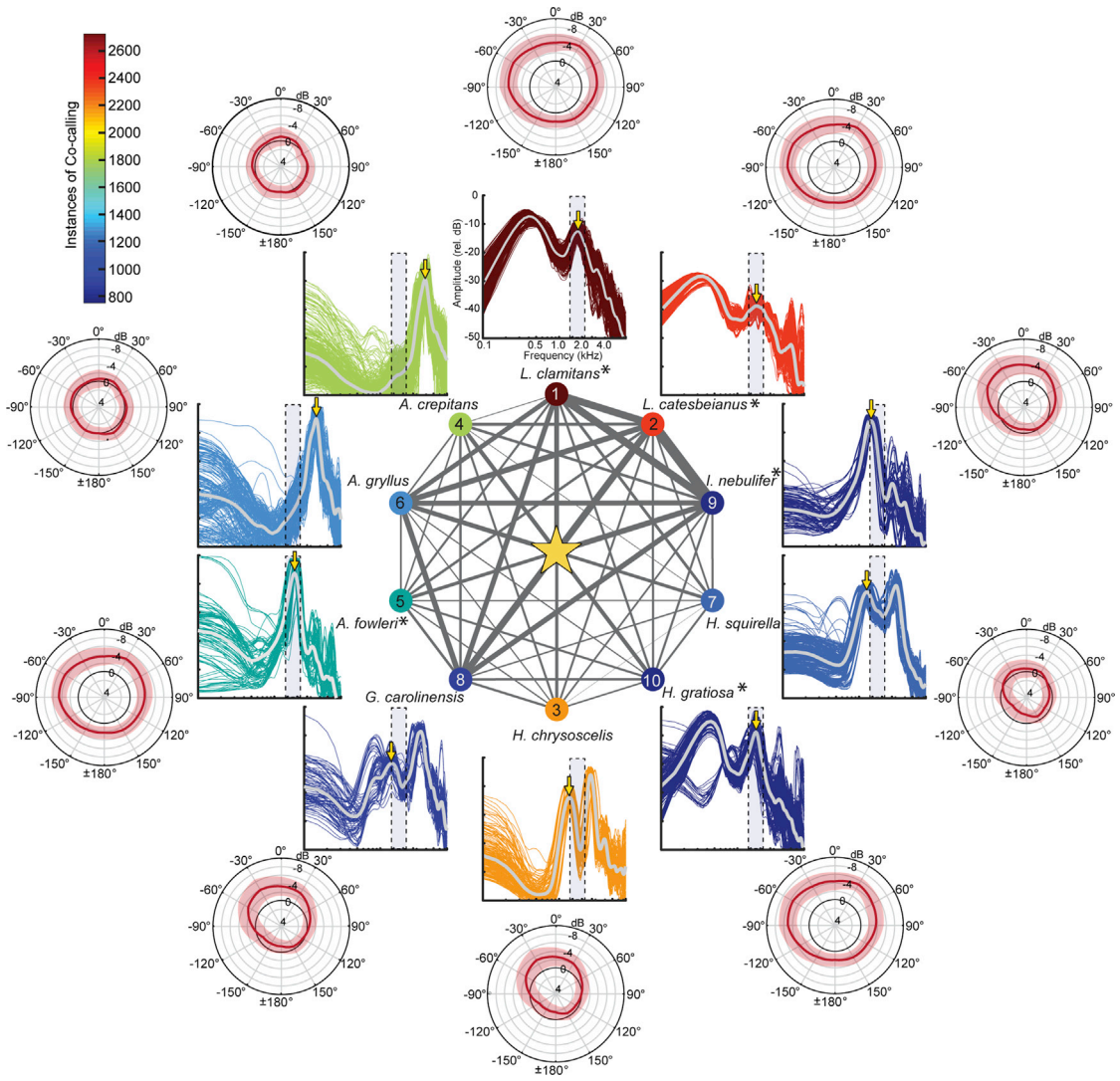

Figure 3. Inflated lungs attenuate tympanum vibrations to heterospecific calls

The central figure depicts the social network of "co-calling" between green treefrogs (*star*) and the top-10 heterospecific species identified to call in multi-species choruses according to the North American Amphibian Monitoring Project (NAAMP; Figure S4). Surrounding the network are depictions of the frequency spectra of each heterospecific species' advertisement calls. Gray lines depict the mean spectrum, averaged over all individuals and calls; colored lines depict the spectrum for each analyzed call and are scaled in color according to the instances of co-calling with green treefrogs (color bar). The shaded blue rectangle in each spectrum represents the frequency range of maximal attenuation of the green treefrog's tympanum vibration amplitude (1400 to 2200 Hz) as a result of lung inflation. Surrounding the spectra are polar plots depicting the mean ± 95% CI attenuation of the spectral peaks indicated by downward pointing yellow arrows when the lungs were inflated versus deflated (n = 21 individuals). Statistical analyses are reported in Table S1 for 5 of the top-10 most commonly encountered heterospecific species that produce calls with acoustic energy attenuated by having inflated lungs.

We then computed the difference between the two states of lung inflation in the amplitude of the spectral peak of each heterospecific species' calls within or closest to the range of 1400 to 2200 Hz.

Inflated lungs attenuated the amplitude of the relevant spectral peaks of these five heterospecific species' calls by approximately −4 to −6 dB on average (Figure 3; Table S1). The greatest lung-mediated reductions in amplitude in the range of 1400 to 2200 Hz occurred for the calls of bullfrogs (*L. catesbeianus*), green frogs (*L. clamitans*), and barking treefrogs (*H. gratiosa*) (Figure 3; Table S1). Notably, bullfrogs and green frogs co-called with green treefrogs most frequently in the NAAMP dataset, with these two heterospecific species alone accounting for 26% of all reported instances of co-calling. Barking treefrogs are the sister species of green treefrogs. The costs of hybrid matings with barking treefrogs have driven evolutionary change in the spectral preferences of female green treefrogs;[55] therefore, mitigating the risk of mis-mating by attenuating the calls of a closely related heterospecific species could be one additional benefit of the lungs' impacts on tympanic responses.

Together, our results suggest inflated lungs improve the signal-to-noise ratio for communication in multi-species frog choruses not by amplifying conspecific signals, but by attenuating the tympanum's response to environmental noise created

Please cite this article in press as: Lee et al., Lung Mediated Auditory Contrast Enhancement Improves the Signal-to-Noise Ratio for Communication in Frogs, Current Biology (2021), https://doi.org/10.1016/j.cub.2021.01.048

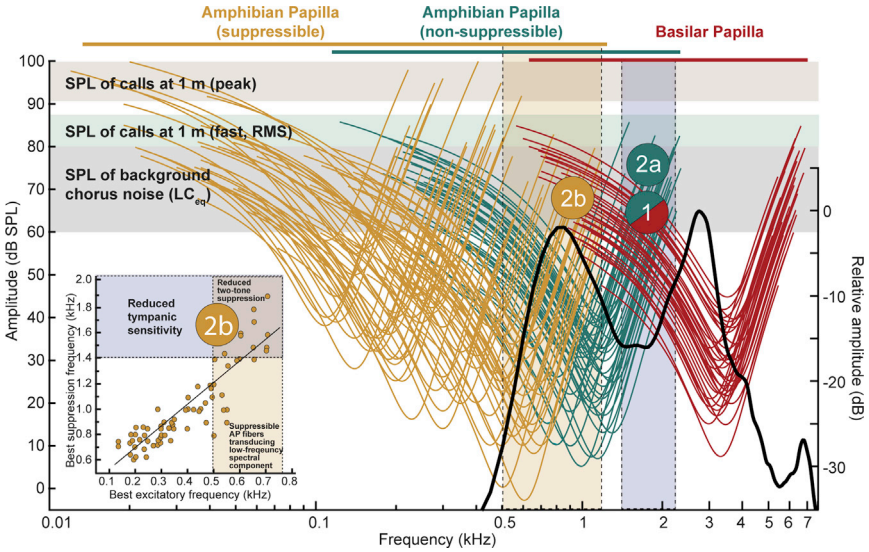

Figure 4. Inflated lungs sharpen peripheral frequency tuning

Modeled tuning curves for 161 auditory nerve fibers in green treefrogs[51] are shown in relation to the frequency range of lung-mediated reductions in tympanum sensitivity (1400 to 2200 Hz, shaded blue rectangle), the spectrum of conspecific calls (solid black line redrawn from Figure 1E), and the sound pressure levels (SPLs) of conspecific advertisement calls[31] and background chorus noise for a closely related treefrog.[59] Tuning curves are depicted separately for suppressible low-frequency and non-suppressible mid-frequency fibers innervating the amphibian papilla (AP) and for high-frequency fibers innervating the basilar papilla (BP). Neural responses of low-frequency fibers innervating the AP can be suppressed by frequencies in the range of mid-frequency AP fibers[60] (see *inset*). As the modeled tuning curves illustrate, suppressible nerve fibers with best excitatory frequencies in the range of approximately 0.5 to 0.7 kHz transduce the low-frequency spectral component of conspecific calls at the high sound amplitudes used for communication (shaded gold rectangle). The model predicts two mechanisms by which attenuating the tympanum response to frequencies between 1400 Hz and 2200 Hz is expected to improve sensory processing of conspecific calls. First, reduced stimulation by environmental noise of both non-suppressible AP fibers and BP fibers at frequencies where their tuning overlaps ('1') should reduce energetic masking of both spectral components in conspecific calls. Second, reduced stimulation of non-suppressible AP fibers ('2a') should additionally reduce two-tone rate suppression of suppressible AP fibers ('2b') that transduce the low-frequency component of the call (see *inset*). (*Inset:* Relationship between best suppression frequency and best excitatory frequency for 70 suppressible auditory nerve fibers derived from the AP [redrawn from Figure 3 in[60]]. Approximately half of the nerve fibers with best excitatory frequencies in the range of 0.5 to 0.7 kHz [shaded gold rectangle] can be suppressed by sound energy in the range of 1.4 to 1.9 kHz, where the lungs attenuate tympanum responses [shaded blue rectangle].)

by the calls of other frog species. To investigate how such an improvement in signal-to-noise ratio at the tympanum might promote improved neural processing of conspecific calls, we assessed the impacts of inflated lungs using a physiological model of peripheral frequency tuning.

Inflated lungs sharpen peripheral frequency tuning

Amphibians are unique among vertebrates in having inner ears with two physically distinct sensory papillae – the amphibian and basilar papillae – that transduce different frequency ranges of airborne sounds. In frogs, these papillae are typically most sensitive to one or more spectral components in conspecific advertisement calls.[27] We modeled peripheral frequency tuning in green treefrogs by estimating frequency tuning curves as 4th order gammatone filters[56] that we parameterized using published data on best excitatory frequencies, bandwidths, and thresholds for 161 auditory nerve fibers in this species[51] (Figure 4). Separate populations of auditory nerve fibers innervating the amphibian papilla are tuned to low frequencies (up to about 700 Hz) and mid-range frequencies (up to about 1300 Hz), whereas a third population of auditory nerve fibers innervating the basilar papilla is more consistently tuned to a common range of higher frequencies (Figure 4). The thresholds of auditory nerve fibers innervating the amphibian and basilar papillae are lowest at frequencies matching, respectively, the low-frequency and high-frequency spectral peaks in the advertisement call (Figure 4), to which the species is also behaviorally most sensitive.[57,58]

The key finding revealed by this physiological model is that lung-mediated impacts on tympanic sensitivity occur in the frequency range where the tuning of the amphibian and basilar papillae can overlap (Figure 4). At low amplitudes near threshold, neither inner ear papilla responds to frequencies between 1400 and 2200 Hz. However, the bandwidth of individual auditory nerve fibers broadens considerably at higher sound levels more typical of communication in natural environments, ultimately causing the tuning of the two inner ear papillae to overlap.[52,61] Much of the frequency range of overlap between the amphibian and basilar papillae at high sound levels corresponds to the frequency range (1400 to 2200 Hz) where notch filtering by inflated lungs attenuates the tympanum's vibration amplitude (Figure 4). Given this correspondence, the modeled tuning of auditory nerve fibers reveals two possible mechanisms by which the subtractive notch filtering generated by inflated lungs could function to counteract the negative impacts of environmental noise in the frequency range of 1400 to 2200 Hz.

First, inflated lungs should reduce energetic masking of conspecific advertisement calls. Consistent with behavioral studies[61] and recordings of auditory brainstem responses,[52] auditory nerve fibers innervating both the mid-frequency region of the amphibian papilla and the basilar papilla respond to frequencies in the range of 1400 to 2200 Hz at high amplitudes typical of communication. Notch filtering by inflated lungs should reduce the ability of environmental noise in this frequency range to drive auditory nerve responses that could otherwise mask neural responses to conspecific calls. Second, notch filtering by inflated lungs should reduce two-tone rate suppression along the amphibian papilla. Two-tone rate suppression is a well-known feature of auditory processing in vertebrates,[62] including green treefrogs,[60,63] whereby neural responses to one frequency are suppressed by the addition of a second frequency. In green treefrogs, suppressible auditory nerve fibers with best

Please cite this article in press as: Lee et al., Lung Mediated Auditory Contrast Enhancement Improves the Signal-to-Noise Ratio for Communication in Frogs, Current Biology (2021), https://doi.org/10.1016/j.cub.2021.01.048

frequencies between approximately 500 and 700 Hz respond to the low-frequency component of conspecific calls at the high amplitudes typical of communication (Figure 4). Importantly, these fibers are suppressed by simultaneous sound energy between approximately 1400 and 2000 Hz (see Figure 4 *inset*).[60,63] Thus, notch filtering that selectively attenuates the tympanum's response in this frequency range should additionally reduce two-tone rate suppression of excitatory neural responses to the lower spectral peaks of conspecific calls. Together, reduced energetic masking and reduced two-tone suppression would provide straightforward mechanisms for realizing at a neurophysiological level any benefits arising from lung-mediated spectral contrast enhancement at the tympanum.

DISCUSSION

The main findings from this study can be summarized as follows. When the lungs were in a naturally inflated state, tympanum vibrations were attenuated within a narrow but biologically important range of frequencies (1400 to 2200 Hz). In response to sound, inflated lungs resonated in the same frequency range where they attenuated tympanum vibrations, and this attenuation was due to indirect sound transmission from the lungs to the internal surface of the tympanum. The tuning of this pulmonary notch filter was consequential: the filter attenuated frequencies that correspond both to the valley between the two spectral peaks of conspecific calls and to the range of spectral overlap in sensitivity between the separate inner ear organs that transduce these two spectral peaks. Consequently, the state of lung inflation had no impact on the tympanum's response to the calls of conspecific males. In contrast, spectral components in the calls of some of the heterospecific frogs most frequently encountered in multi-species choruses were significantly attenuated by the pulmonary notch filter. Together, these findings for green treefrogs support the SCE hypothesis and suggest the frog's lungs serve a heretofore unknown noise-control function in vertebrate hearing and sound communication.

To what extent do results from green treefrogs generalize to other frog species? Relevant comparative data are available from three families of frogs (Hylidae, Ranidae, and Eleutherodactylidae) belonging to two superfamilies that last shared a common ancestor some 155 million years ago (Hyloidea: Hylidae and Eleutherodactylidae; Ranoidea: Ranidae). Studies of these species suggest the *relative* relationships reported here for green treefrogs between lung resonance frequency and the frequencies of the spectral peaks and valleys of conspecific calls is taxonomically widespread in frogs.[40,43] That is, across distantly related frog species in three different families, the lung resonance frequency falls within the valley between the spectral peaks of advertisement calls. Across species, we would generally expect lung resonance frequency, call frequencies, and also peripheral frequency tuning to covary in a coordinated fashion as a function of species differences in body size, because larger frogs have lungs of greater volume (and hence lower lung resonance frequencies) and larger vocal folds (and hence lower call frequencies). Our results, together with these comparative data, suggest the hypothesis that spectral contrast enhancement may be common among the more than 7200 species of frog in Order Anura.

We suggest the frog's lung-to-ear sound transmission pathway helps mitigate noise problems in multi-species breeding choruses. For humans, following speech in a noisy social gathering (i.e., solving the cocktail party problem) typically means contending with the sounds generated by other vocalizing conspecifics.[25] But many nonhuman animals, like frogs, communicate in large aggregations where the sounds of other species create prominent sources of noise and overlapping signals.[10,24] Species that breed in such aggregations can be under intense selection to solve cocktail-party-like problems because accurate perception of acoustic sexual signals is tightly linked to evolutionary fitness.[21–24] The negative impacts of auditory masking caused by background noise and overlapping signals should, thus, favor the evolution of adaptive mechanisms that promote more effective communication in noise. One such adaptation in frogs is for signalers of different species to call at different frequencies, thereby partitioning the limited spectral bandwidth in multi-species choruses ("acoustic niche partitioning").[64,65] On the receiver side, the benefits of lung-mediated spectral contrast enhancement would complement spectral partitioning by further reducing the potential for other species' calls to disrupt communication.

To our knowledge, lung-to-ear sound transmission in frogs represents a novel mechanism by which nature has attempted to solve the general biological problem of hearing and communicating in noise. This finding has three broad implications. First, it demonstrates the extraordinary power of evolution to co-opt pre-existing adaptations for new functions. Resonances of air-filled structures such as lungs or swim bladders improve sound detection in aquatic vertebrates,[66] and sound detection via the lungs also played important roles in hearing during the evolutionary transition of vertebrates from water to land.[67] Thus, it is likely that the lungs of the earliest terrestrial vertebrates functioned as accessory sound receiving structures prior to the subsequent evolution of tympanic middle ears[29] and vocal communication.[30] Our results suggest evolution co-opted this ancient amphibian adaptation for sound reception through the lungs—structures already adapted for respiring in air—to provide spectral contrast enhancement that improves the signal-to-noise ratio for communication in extant frogs.

Second, the noise control function of lung-to-ear sound transmission in frogs illustrates how evolution precedes human engineers in finding clever solutions to common problems. People with sensorineural hearing loss, for example, have significant problems understanding speech in noisy social settings. Digital algorithms for SCE can produce 2 to 4 dB improvements in signal-to-noise ratio that yield significantly better word recognition and response times in hearing impaired listeners.[48] Some SCE algorithms that improve speech recognition for cochlear implant users do so by attenuating the valleys between the peaks of formant frequencies in the speech spectrum without altering the levels of the peaks themselves.[47] This human engineering solution is functionally analogous to how inflated lungs impact tympanic sensitivity in frogs: the state of lung inflation had no impact on the formant-like spectral peaks present in conspecific calls, but inflated lungs attenuated the tympanum's response to frequencies in the valley between them. Attenuation of −4 to −6 dB was common, with the maximum attenuation averaging approximately −10 dB. Previous studies of auditory

masking in frogs suggest an enhancement of spectral contrast that improved signal-to-noise ratios on the order of 4 to 10 dB or more could yield substantial benefits in terms of improved call detection, recognition, and discrimination in noise.[22] Our physiological model of peripheral frequency tuning suggests these benefits could arise due to lung-mediated reductions in both energetic masking and two-tone suppression of neural responses to conspecific calls.

Finally, results from the present study resolve a long-standing paradox in comparative research on vertebrate hearing. An early hypothesis for the function of lung-to-ear sound transmission in frogs was that it sharpens the inherent directionality of their internally coupled ears.[35–39] Increased directionality at conspecific call frequencies would presumably confer selective advantages in locating calling males in the dark and physically complex environment of a nighttime chorus. Previous studies of frogs,[36–38,40] including green treefrogs,[43] indicate lung-to-ear sound transmission sharpens directional tuning at frequencies near the lung resonance frequency with very little (if any) impact on directionality at frequencies used for social and sexual communication with conspecifics. Moreover, sound localization worsens at frequencies near the lung resonance,[37] presumably because the lung input fails to enhance binaural comparisons of directional information.[43] Our findings finally resolve this apparent paradox by emphasizing that it is the frequency- and direction-dependent, lung-mediated reduction in tympanic sensitivity—and not the associated increase in directionality—that plays a functional role in hearing and sound communication in frogs. A more recent hypothesis for the function of the lung-to-ear pathway is that it protects a male frog's hearing while vocalizing.[41] That the lungs might play a role in hearing protection for signalers during active calling is compatible with their role in spectral contrast enhancement for receivers during passive listening.

In conclusion, we propose natural selection has acted to exploit a preexisting lung-to-ear coupling to facilitate perception of conspecific calls in noisy social environments by providing a mechanism for real-time spectral contrast enhancement at the auditory periphery. This conclusion broadens our understanding of the diversity of evolutionary adaptations to noise in nonhuman animals as well as the function of a unique sound transmission pathway in one of the most vocal groups of extant vertebrates. At present, the precise physical mechanism by which a sound-induced lung resonance attenuates sound-induced tympanum vibrations remains unknown and requires further investigation. We speculate that amplitude- and phase-dependent interactions between indirect sound transmission from the lungs and contralateral tympanum and direct sound input to the tympanum's external surface result in frequency- and direction-dependent destructive interference that selectively attenuates tympanum vibrations. If so, then sound transmission via the lungs and internally coupled tympanum would constitute a biological mechanism for noise cancellation that is functionally analogous to signal processing strategies implemented in noise-cancellation headphones.[68]

STAR★METHODS

Detailed methods are provided in the online version of this paper and include the following:

SUPPLEMENTAL INFORMATION

Supplemental Information can be found online at https://doi.org/10.1016/j.cub.2021.01.048.

ACKNOWLEDGMENTS

We thank Eric Cole, Carl Gerhardt, Saumya Gupta, Lata Kalra, Katie LaBarbera, Hongyu Li, Marlene Zuk, and three anonymous referees for feedback on the manuscript; Jesse Tanner and Mary Elson for help collecting frogs; Saumya Gupta for assistance with animal husbandry; and the Texas Parks and Wildlife Division for permission to collect frogs (SPR-0410-054). The contents in this article are those of the authors and do not necessarily reflect the view of the U.S. President's Emergency Plan for AIDS Relief, the U.S. Agency for International Development or the U.S. Government. Funding was provided by a grant from the U.S. National Science Foundation to M.A.B. (IOS-1452831).

AUTHOR CONTRIBUTIONS

Conceptualization, N.L., J.C-D, M.A.B; Methodology, N.L., J.C-D, M.A.B; Software, N.L.; Investigation, N.L., J.C-D, K.M.S., M.A.B; Resources, N.L., M.A.B.; Data Curation, N.L., M.A.B.; Writing – Original Draft, M.A.B.; Writing – Review & Editing, N.L., J.C-D, L.A.W., K.M.S., M.A.B; Visualization, N.L., J.C-D, L.A.W., M.A.B; Funding Acquisition, M.A.B.

DECLARATION OF INTERESTS

The authors declare no competing interests.

Received: November 2, 2020
Revised: December 23, 2020
Accepted: January 13, 2021
Published: March 4, 2021

REFERENCES

1. Diambra, L., and Santillan, M. (2019). Emergent effects of noise in biology: from gene expression to cell motility. Front. Phys. *7*, https://doi.org/10.3389/fphy.2019.00083.
2. Tsimring, L.S. (2014). Noise in biology. Rep. Prog. Phys. *77*, 026601.
3. Ladbury, J.E., and Arold, S.T. (2012). Noise in cellular signaling pathways: causes and effects. Trends Biochem. Sci. *37*, 173–178.
4. Kontogeorgaki, S., Sánchez-García, R.J., Ewing, R.M., Zygalakis, K.C., and MacArthur, B.D. (2017). Noise-processing by signaling networks. Sci. Rep. *7*, 532.

5. Chalancon, G., Ravarani, C.N., Balaji, S., Martinez-Arias, A., Aravind, L., Jothi, R., and Babu, M.M. (2012). Interplay between gene expression noise and regulatory network architecture. Trends Genet. *28*, 221–232.
6. Bandiera, L., Furini, S., and Giordano, E. (2016). Phenotypic variability in synthetic biology applications: dealing with noise in microbial gene expression. Front. Microbiol. *7*, https://doi.org/10.3389/fmicb.2016.00479.
7. Faisal, A.A., Selen, L.P.J., and Wolpert, D.M. (2008). Noise in the nervous system. Nat. Rev. Neurosci. *9*, 292–303.
8. McDonnell, M.D., and Ward, L.M. (2011). The benefits of noise in neural systems: bridging theory and experiment. Nat. Rev. Neurosci. *12*, 415–426.
9. Brumm, H., and Slabbekoorn, H. (2005). Acoustic communication in noise. Adv. Stud. Behav. *35*, 151–209.
10. H. Brumm, ed. (2013). Animal Communication and Noise (New York: Springer).
11. Wiley, R.H. (2015). Noise Matters: The Evolution of Communication (Cambridge, MA: Harvard University Press).
12. Aubin, T., and Jouventin, P. (2002). How to vocally identify kin in a crowd: The penguin model. Adv. Stud. Behav. *31*, 243–277.
13. Ryan, M.J., Akre, K.L., and Kirkpatrick, M. (2007). Mate choice. Curr. Biol. *17*, R313–R316.
14. Gomes, D.G.E., Page, R.A., Geipel, I., Taylor, R.C., Ryan, M.J., and Halfwerk, W. (2016). Bats perceptually weight prey cues across sensory systems when hunting in noise. Science *353*, 1277–1280.
15. Pohl, N.U., Slabbekoorn, H., Klump, G.M., and Langemann, U. (2009). Effects of signal features and environmental noise on signal detection in the great tit, *Parus major*. Anim. Behav. *78*, 1293–1300.
16. Lee, N., and Mason, A.C. (2017). How spatial release from masking may fail to function in a highly directional auditory system. eLife *6*, e20731.
17. Reichert, M.S., and Ronacher, B. (2015). Noise affects the shape of female preference functions for acoustic signals. Evolution *69*, 381–394.
18. Lohr, B., Wright, T.F., and Dooling, R.J. (2003). Detection and discrimination of natural calls in masking noise by birds: estimating the active space of a signal. Anim. Behav. *65*, 763–777.
19. Dominoni, D.M., Halfwerk, W., Baird, E., Buxton, R.T., Fernández-Juricic, E., Fristrup, K.M., McKenna, M.F., Mennitt, D.J., Perkin, E.K., Seymoure, B.M., et al. (2020). Why conservation biology can benefit from sensory ecology. Nat. Ecol. Evol. *4*, 502–511.
20. Slabbekoorn, H., Dooling, R.J., Fay, R.R., and Popper, A.N. (2018). Effects of Anthropogenic Noise on Animals (New York: Springer).
21. Römer, H. (2013). Masking by noise in acoustic insects: Problems and solutions. In Animal Communication and Noise, H. Brumm, ed. (New York: Springer), pp. 33–63.
22. Bee, M.A. (2015). Treefrogs as animal models for research on auditory scene analysis and the cocktail party problem. Int. J. Psychophysiol. *95*, 216–237.
23. Klump, G.M. (2016). Perceptual and neural mechanisms of auditory scene analysis in the European starling. In Psychological Mechanisms in Animal Communication, M.A. Bee, and C.T. Miller, eds. (Cham, Switzerland: Springer), pp. 57–88.
24. Bee, M.A., and Micheyl, C. (2008). The cocktail party problem: What is it? How can it be solved? And why should animal behaviorists study it? J. Comp. Psychol. *122*, 235–251.
25. McDermott, J.H. (2009). The cocktail party problem. Curr. Biol. *19*, R1024–R1027.
26. Middlebrooks, J.C., Simon, J.Z., Popper, A.N., and Fay, R.R. (2017). The Auditory System at the Cocktail Party (Berlin: Springer).
27. Gerhardt, H.C., and Huber, F. (2002). Acoustic Communication in Insects and Anurans: Common Problems and Diverse Solutions (Chicago: Chicago University Press).
28. Feng, A.S., and Schul, J. (2007). Sound processing in real-world environments. In Hearing and Sound Communication in Amphibians, P.A. Narins, A.S. Feng, R.R. Fay, and A.N. Popper, eds. (New York: Springer), pp. 323–350.
29. Clack, J.A., and Allin, E. (2004). The evolution of single-and multiple-ossicle ears in fishes and tetrapods. In Evolution of the Vertebrate Auditory System, *Volume 22*, G.A. Manley, A.N. Popper, and R.R. Fay, eds. (New York: Springer), pp. 128–163.
30. Chen, Z., and Wiens, J.J. (2020). The origins of acoustic communication in vertebrates. Nat. Commun. *11*, https://doi.org/10.1038/s41467-020-14356-3.
31. Gerhardt, H.C. (1975). Sound pressure levels and radiation patterns of vocalizations of some North American frogs and toads. J. Comp. Physiol. *102*, 1–12.
32. Arak, A. (1983). Sexual selection by male-male competition in natterjack toad choruses. Nature *306*, 261–262.
33. Narins, P.M. (1982). Effects of masking noise on evoked calling in the Puerto Rican coqui (Anura, Leptodactylidae). J. Comp. Physiol. *147*, 439–446.
34. Tanner, J.C., and Bee, M.A. (2020). Inconsistent sexual signaling degrades optimal mating decisions in animals. Science Advances *6*, https://doi.org/10.1126/sciadv.aax3957.
35. Narins, P.M., Ehret, G., and Tautz, J. (1988). Accessory pathway for sound transfer in a neotropical frog. Proc. Natl. Acad. Sci. USA *85*, 1508–1512.
36. Jørgensen, M.B. (1991). Comparative studies of the biophysics of directional hearing in anurans. J. Comp. Physiol. A Neuroethol. Sens. Neural Behav. Physiol. *169*, 591–598.
37. Jørgensen, M.B., and Gerhardt, H.C. (1991). Directional hearing in the gray tree frog *Hyla versicolor:* eardrum vibrations and phonotaxis. J. Comp. Physiol. A Neuroethol. Sens. Neural Behav. Physiol. *169*, 177–183.
38. Jørgensen, M.B., Schmitz, B., and Christensen-Dalsgaard, J. (1991). Biophysics of directional hearing in the frog *Eleutherodactylus coqui*. J. Comp. Physiol. A Neuroethol. Sens. Neural Behav. Physiol. *168*, 223–232.
39. Ehret, G., Keilwerth, E., and Kamada, T. (1994). The lung-eardrum pathway in three treefrog and four dendrobatid frog species: some properties of sound transmission. J. Exp. Biol. *195*, 329–343.
40. Bee, M.A., and Christensen-Dalsgaard, J. (2016). Sound source localization and segregation with internally coupled ears: the treefrog model. Biol. Cybern. *110*, 271–290.
41. Narins, P.M. (2016). ICE on the road to auditory sensitivity reduction and sound localization in the frog. Biol. Cybern. *110*, 263–270.
42. De Jongh, H., and Gans, C. (1969). On the mechanism of respiration in the bullfrog, *Rana catesbeiana*: A reassessment. J. Morphol. *127*, 259–289.
43. Christensen-Dalsgaard, J., Lee, N., and Bee, M.A. (2020). Lung-to-ear sound transmission does not improve directional hearing in green treefrogs (*Hyla cinerea*). J. Exp. Biol. *223*, jeb232421.
44. Fletcher, N.H., and Rossing, T.D. (2012). The Physics of Musical Instruments (New York: Springer).
45. Barron, R.F. (2003). Industrial Noise Control and Acoustics (New York, NY: Marcel Dekker, Inc.).
46. Fletcher, N.H. (1992). Acoustic Systems in Biology (Oxford University Press).
47. Nogueira, W., Rode, T., and Büchner, A. (2016). Spectral contrast enhancement improves speech intelligibility in noise for cochlear implants. J. Acoust. Soc. Am. *139*, 728–739.
48. Baer, T., Moore, B.C., and Gatehouse, S. (1993). Spectral contrast enhancement of speech in noise for listeners with sensorineural hearing impairment: effects on intelligibility, quality, and response times. J. Rehabil. Res. Dev. *30*, 49–72.
49. Simpson, A.M., Moore, B.C.J., and Glasberg, B.R. (1990). Spectral enhancement to improve the intelligibility of speech in noise for hearing-impaired listeners. Acta Otolaryngol. *109* (sup469), 101–107.
50. Lee, N., Schrode, K.M., and Bee, M.A. (2017). Nonlinear processing of a multicomponent communication signal by combination-sensitive neurons

in the anuran inferior colliculus. J. Comp. Physiol. A Neuroethol. Sens. Neural Behav. Physiol. *203*, 749–772.

51. Ehret, G., and Capranica, R.R. (1980). Masking patterns and filter characteristics of auditory nerve fibers in the green treefrog (*Hyla cinerea*). J. Comp. Physiol. *141*, 1–12.
52. Buerkle, N.P., Schrode, K.M., and Bee, M.A. (2014). Assessing stimulus and subject influences on auditory evoked potentials and their relation to peripheral physiology in green treefrogs (*Hyla cinerea*). Comp. Biochem. Physiol. A Mol. Integr. Physiol. *178*, 68–81.
53. Weir, L.A., and Mossman, M.J. (2005). North American Amphibian Monitoring Program (NAAMP). In Amphibian Declines: Conservation Status of United States Species, M.J. Lannoo, ed. (Berkeley: University of California Press), pp. 307–313.
54. Foreman, T.M., Grant, E.H.C., and Weir, L.A. (2017). North American Amphibian Monitoring Program (NAAMP) anuran detection data from the eastern and central United States (1994-2015). U.S. Geological Survey data release. https://doi.org/10.5066/F7G44NG0.
55. Höbel, G., and Gerhardt, H.C. (2003). Reproductive character displacement in the acoustic communication system of green tree frogs (*Hyla cinerea*). Evolution *57*, 894–904.
56. Lee, N., Ward, J.L., Vélez, A., Micheyl, C., and Bee, M.A. (2017). Frogs exploit statistical regularities in noisy acoustic scenes to solve cocktail-party-like problems. Curr. Biol. *27*, 743–750.
57. Moss, C.F., and Simmons, A.M. (1986). Frequency selectivity of hearing in the green treefrog, *Hyla cinerea*. J. Comp. Physiol. A Neuroethol. Sens. Neural Behav. Physiol. *159*, 257–266.
58. Megela-Simmons, A., Moss, C.F., and Daniel, K.M. (1985). Behavioral audiograms of the bullfrog (*Rana catesbeiana*) and the green tree frog (*Hyla cinerea*). J. Acoust. Soc. Am. *78*, 1236–1244.
59. Tanner, J.C., and Bee, M.A. (2019). Within-individual variation in sexual displays: signal or noise? Behav. Ecol. *30*, 80–91.
60. Ehret, G., Moffat, A.J.M., and Capranica, R.R. (1983). Two-tone suppression in auditory nerve fibers of the green treefrog (*Hyla cinerea*). J. Acoust. Soc. Am. *73*, 2093–2095.
61. Gerhardt, H.C. (2005). Acoustic spectral preferences in two cryptic species of grey treefrogs: implications for mate choice and sensory mechanisms. Anim. Behav. *70*, 39–48.
62. Sachs, M.B., Young, E.D., and Lewis, R.H. (1974). Discharge patterns of single fibers in the pigeon auditory nerve. Brain Res. *70*, 431–447.
63. Gerhardt, H.C., and Höbel, G. (2005). Mid-frequency suppression in the green treefrog (*Hyla cinerea*): mechanisms and implications for the evolution of acoustic communication. J. Comp. Physiol. A Neuroethol. Sens. Neural Behav. Physiol. *191*, 707–714.
64. Garcia-Rutledge, E.J., and Narins, P.M. (2001). Shared acoustic resources in an old world frog community. Herpetologica *57*, 104–116.
65. Villanueva-Rivera, L.J. (2014). Eleutherodactylus frogs show frequency but no temporal partitioning: implications for the acoustic niche hypothesis. PeerJ *2*, e496. https://doi.org/10.7717/peerj.496.
66. Popper, A.N., and Fay, R.R. (2011). Rethinking sound detection by fishes. Hear. Res. *273*, 25–36.
67. Christensen, C.B., Christensen-Dalsgaard, J., and Madsen, P.T. (2015). Hearing of the African lungfish (*Protopterus annectens*) suggests underwater pressure detection and rudimentary aerial hearing in early tetrapods. J. Exp. Biol. *218*, 381–387.
68. Kuo, S.M., and Morgan, D.R. (1999). Active noise control: A tutorial review. Proc. IEEE *87*, 943–973.
69. Caldwell, M.S., Lee, N., Schrode, K.M., Johns, A.R., Christensen-Dalsgaard, J., and Bee, M.A. (2014). Spatial hearing in Cope's gray treefrog: II. Frequency-dependent directionality in the amplitude and phase of tympanum vibrations. J. Comp. Physiol. A Neuroethol. Sens. Neural Behav. Physiol. *200*, 285–304.
70. Bee, M., Kozich, C., Blackwell, K., and Gerhardt, H. (2001). Individual variation in advertisement calls of territorial male green frogs, *Rana clamitans*: implications for individual discrimination. Ethology *107*, 65–84.
71. Bee, M., and Gerhardt, H. (2001). Neighbour-stranger discrimination by territorial male bullfrogs (Rana catesbeiana): I. Acoustic basis. Anim. Behav. *62*, 1129–1140.
72. Csardi, G., and Nepusz, T. (2006). The igraph software package for complex network research. InterJournal. Complex Syst. *1695*, 1–9.
73. Patterson, R.D., Nimmo-Smith, I., Holdsworth, J., and Rice, P. (1987). An efficient auditory filterbank based on the gammatone function. In A Meeting of the IOC Speech Group on Auditory Modelling at RSRE, Volume 2.
74. Hohmann, V. (2002). Frequency analysis and synthesis using a Gammatone filterbank. Acta Acust. United Acust. *88*, 433–442.
75. Tummers, B. (2006). DataThief III. Volume 2020.

Please cite this article in press as: Lee et al., Lung Mediated Auditory Contrast Enhancement Improves the Signal-to-Noise Ratio for Communication in Frogs, Current Biology (2021), https://doi.org/10.1016/j.cub.2021.01.048

STAR★METHODS

KEY RESOURCES TABLE

REAGENT or RESOURCE	SOURCE	IDENTIFIER
Antibodies		
Bacterial and Virus Strains		
Biological Samples		
Chemicals, Peptides, and Recombinant Proteins		
Critical Commercial Assays		
Deposited Data		
Experimental Models: Cell Lines		
Experimental Models: Organisms/Strains		
Female green treefrogs, *Hyla cinerea*	Wild caught	NA
Oligonucleotides		
Recombinant DNA		
Software and Algorithms		
Statistical analysis SPSS	IBM Corp. Released 2012. IBM SPSS Statistics for Windows, Version 21.0. Armonk, NY: IBM Corp.	Version 21
MATLAB	Mathworks, Natick, MA	Versions 2014a, 2020a
StimProg	Norman Lee	Version 6
Other		
Laser vibrometer	Polytech, Irvine, CA	PDV-100

RESOURCE AVAILABILITY

Lead Contact

Further information and requests for resources and data should be directed to and will be fulfilled by the Lead Contact, Norman Lee (lee33@stolaf.edu).

Materials availability

This study did not generate new unique reagents.

Data and code availability

The datasets generated and analyzed during the current study have been deposited to Mendeley Data: https://dx.doi.org/10.17632/9d35jf2zjz.1. Code used to analyze the laser vibrometry and bioacoustic data are available upon reasonable request and should be directed to and will be fulfilled by the Lead Contact, Norman Lee (lee33@stolaf.edu). All code and data used to generate the social network figures are available at: https://github.com/whit1951/FrogNetworks.

EXPERIMENTAL MODEL AND SUBJECT DETAILS

Animals

Subjects were 25 female green treefrogs collected on the grounds of the East Texas Conservation Center in Jasper County, Texas, U.S.A. (30°56'46.15"N, 94°7'51.46"W). Animals were housed in the laboratory at the University of Minnesota on a 12 h photoperiod, provided with access to perches and refugia, fed a diet of vitamin-dusted crickets, and given *ad libitum* access to fresh water. All procedures were approved by the Institutional Animal Care and Use Committees of the University of Minnesota (#1401-31258A) and complied with the NIH *Guide for the Care and Use of Laboratory Animals* (8th Edition).

Please cite this article in press as: Lee et al., Lung Mediated Auditory Contrast Enhancement Improves the Signal-to-Noise Ratio for Communication in Frogs, Current Biology (2021), https://doi.org/10.1016/j.cub.2021.01.048

METHOD DETAILS

Laser vibrometry measurements

We took laser measurements of 25 frogs (snout-to-vent length [SVL]: mean = 54.0 mm, range = 47.7 to 59.2 mm; mass: mean = 12.5 g, range = 8.3 to 17.6 g). For laser measurements, subjects were immobilized with succinylcholine chloride (5 μg/g). Over the 5-10 min during which the immobilizing agent took effect, subjects were allowed to regulate their own lung volume. After full immobilization was achieved, lung ventilation had stopped and lung inflation (based on body wall extension) resembled that observed for unmanipulated frogs sitting in a natural posture.[69] We refer to this state of lung inflation as ''inflated.'' For some procedures, we also examined animals in one or two additional states of lung inflation that involved manually deflating and reinflating the lungs. To create a ''deflated'' condition, we expressed the air in the animal's lungs by gently depressing the lateral body wall while holding the glottis open with the narrow end of a small, plastic pipette tip. We created a ''reinflated'' condition by gently blowing air by mouth through a pipette with its tip located just above the closed glottis; the movement of air was sufficient to open the glottis and inflate the lungs. We made every attempt to return the lungs to the natural level of inflation observed prior to manual deflation. When individuals were measured in multiple conditions, we always made measurements in the inflated condition first followed by the deflated condition and then the reinflated condition. While animals were immobilized, we periodically applied water to the dorsum to keep the skin moist to facilitate cutaneous respiration. All laser measurements of an individual subject were made during a single recording session of less than two hours. (Note that temporary manipulations of lung ventilation are possible in immobilized frogs because amphibians are capable of cutaneous gas exchange.) We excluded four animals from further analyses (final n = 21) because we could not visually confirm their state of lung inflation across treatments at the time measurements were made.

We conducted our experiments in a custom-built, semi-anechoic sound chamber with inside dimensions (L × W × H) of 2.9 m × 2.7 m × 1.9 m (Industrial Acoustics Company, North Aurora, IL). To reduce reverberations inside the chamber, the walls and ceiling were lined with Sonex acoustic foam panels (Model VLW-60; Pinta Acoustic, Inc. Minneapolis, MN). The floor of the chamber was covered in low-pile carpet. During recordings, subjects were positioned on a 30-cm tall pedestal made from wire mesh (0.9-mm diameter wire, 10.0-mm grid spacing). The tip of the subject's mandible rested on a raised arch of thin wire, so that the animal sat in a typical posture in the horizontal plane with its jaw parallel to the ground and its head raised and in line with its body. The bottom of the pedestal was suspended 90 cm above the floor of the chamber using a horizontal, 70-cm long piece of Unistrut® attached to its base (Unistrut, Harvey, IL). The Unistrut beam was mounted to a vibration isolation table (Technical Manufacturing Corporation, Peabody, MA) located against an inside wall of the chamber. The Unistrut and vibration isolation table were covered with the same acoustic foam that lined the walls and ceiling of the chamber.

We measured the vibration amplitude of the animal's right tympanum or body wall using a laser vibrometer (PDV-100, Polytech, Irvine, CA). The laser was mounted on the same vibration isolation table from which the subject pedestal was mounted. We positioned the laser at approximately 70° to the animal's right relative to the direction in which its snout pointed, which we consider to be 0° (Figure S1). To enhance reflectance of the laser, a small (45 – 63 μm diameter), retroreflective glass bead (P-RETRO-500, Polytech, Irvine, CA) was placed at the center of the right tympanum or a position on the right, lateral body wall overlying the lung. The analog output of the laser was acquired (44.1 kHz, 16 bit) using an external digital and analog data acquisition (DAQ) device (NI USB 6259, National Instruments, Austin, TX) that was controlled by custom software written in MATLAB (v.2014a, MathWorks, Natick, MA) and running on an OptiPlex 745 PC (Dell, Round Rock, TX). The spectra of the acquired laser signals were calculated in MATLAB using the pwelch function (window size = 256, overlap = 50%). Laser spectra were corrected for small directional variation in the sound spectrum by subtracting (in dB) the spectrum recorded from a probe microphone (see below) from that of the acquired laser signal. In generating the heatmaps of tympanum responses in Figure 1, we used linear interpolation to determine vibration amplitude values at angles of sound incidence between those measured. Data between measurement points in polar plots were interpolated using a cubic spline.

Free-field acoustic stimulation

Acoustic stimuli (44.1 kHz, 16-bit) were broadcast using the same software and hardware used to acquire the laser signal. We controlled signal levels for calibration and playback using a programmable attenuator (PA5, Tucker-Davis Technologies, Alachua, FL). The stimulus consisted of a frequency-modulated (FM) sweep that was 195 ms in duration, had linear onset and offset ramps of 10 ms, and linearly increased in frequency from 0.2 to 7.5 kHz over the 175-ms steady-state portion of its amplitude envelope. Responses were averaged over 20 repetitions of the stimulus. During measurements with the laser, we also recorded acoustic stimuli by positioning the tip of a probe tube of a G.R.A.S. 40SC probe microphone (G.R.A.S. Sound & Vibration A/S, Holte, Denmark) approximately 2 mm from the position on the animal's body (e.g., the right tympanum or its right body wall) from which the laser recorded the response. The microphone's output was amplified using an MP-1 microphone pre-amplifier (Sound Devices, Reedsburg, WI) and recorded using the NIDAQ device.

For free-field acoustic stimulation (Figure S1A, S1B), the stimulus was amplified (Crown XLS1000, Elkhart, IN) and broadcast through a speaker (Mod1, Orb Audio, New York, NY) located 50 cm away from the approximate center of a subject's head (measured along the interaural axis) as it sat on the pedestal. The speaker was attached to a rotating arm covered in acoustic foam and suspended from the ceiling of the sound chamber so that the center of the speaker was at the same height above the chamber floor as the subject and could be placed at any azimuthal position. We presented the stimulus from 12 different angles around the animal (0° to 330° in 30° steps; Figure S1A). An angle of 0° corresponded to the direction in which the animal's snout pointed; +90

Please cite this article in press as: Lee et al., Lung Mediated Auditory Contrast Enhancement Improves the Signal-to-Noise Ratio for Communication in Frogs, Current Biology (2021), https://doi.org/10.1016/j.cub.2021.01.048

corresponded to the animal's right side (ipsilateral to the laser); and −90° corresponded to the animal's left side (contralateral to the laser). For a given subject, we first recorded responses from the tympanum in the inflated condition. We began recordings at a randomly determined location around the subject and then recorded responses at each successive angle after repositioning the speaker in a counterclockwise direction. After making a recording from the 12th and final speaker location, we deflated the lungs and remeasured the tympanum beginning at the same randomly determined starting location used in the naturally inflated condition. For a subset of 10 subjects (SVL: mean = 54.4 mm, range = 47.7 to 59.2 mm; mass: mean = 13.1 g, range = 8.3 to 17.6 g), we also measured the vibration amplitude of the body wall overlying the lungs in the inflated and deflated states, as well as after manually reinflating the lungs, with the speaker positioned at +90° (Figure S1B). We calibrated the FM sweep to be 85 dB SPL (sound pressure level re 20 μPa, fast, C-weighted) for each speaker position using a Brüel & Kjær Type 2250 sound level meter (Brüel & Kjær Sound & Vibration Measurement A/S, Nærum, Denmark) and a Brüel & Kjær Type 4189 1/2-inch condenser microphone. For calibration, we suspended the microphone from the ceiling of the sound chamber by an extension cable (AO-0414-D-100) so that it hung at the position a subject's head occupied during recordings.

Transmission gain measurements and free-field reconstructions

We used laser vibrometry and local acoustic stimulation of the tympana and body wall to measure the transmission gain of sound input to the tympanum's internal surface via the internally coupled tympanum and the lungs. For local acoustic stimulation (Figure S1C), we broadcast the same FM sweep used in free-field stimulations through a Sony MDREX15LP earbud (Sony Corporation of America, New York, NY) positioned within approximately 2 mm of either the right tympanum (ipsilateral to the laser), the left tympanum (contralateral to the laser), or the left body wall overlying the left lung (contralateral to the laser) (Figure S1C). The opening of the earbud was approximately the same diameter as the tympanum. The earbud was positioned using micromanipulators attached to a ring stand placed on the floor of the sound chamber. The tip of a metal probe tube connected to the G.R.A.S. 40SC probe microphone was inserted through the hybrid silicone of the earbud such that its opening barely protruded into the space between the speaker and the acoustically stimulated tympanum or body wall. The output of the probe microphone was amplified with the MP-1 microphone preamplifier and recorded with the NIDAQ data acquisition device. At each location of stimulation, we determined the mean vibration amplitude averaged over response to 20 repetitions of the stimulus with the lungs in the inflated condition.

Transmission gains were computed as follows. For each location of stimulation (Figure S1C), we first computed a transfer function by dividing the average vibration spectrum of the right (ipsilateral) tympanum's response recorded with the laser by the average sound spectrum at each location recorded with the probe microphone. Thus, separate transfer functions were computed for stimulation of the right tympanum (ipsilateral to the laser; $H_I(\omega)$), the left tympanum (contralateral to the laser; $H_C(\omega)$), and the body wall above the lung (contralateral to the laser; $H_L(\omega)$). From these transfer functions, we then computed the transmission gain for sound input to the internal surface of the ipsilateral tympanum via the contralateral tympanum as $TG_C = H_C(\omega) / H_I(\omega)$ and via the lungs-to-ear pathway as $TG_L = H_L(\omega) / H_I(\omega)$.

Transfer functions measured with local acoustic stimulation allowed us to reconstruct the tympanum's free-field response to sound. To accomplish this, we added the sounds arriving at the tympanum's internal surface via the internally coupled, contralateral tympanum, and via the lung-to-ear pathway to the sound measured at the external surface of the tympanum. The sound arriving via the contralateral tympanum was computed as the sound impinging on the external surface of the contralateral tympanum (measured with the probe microphone) multiplied by the transmission gain of the contralateral tympanum (TG_C). The sound arriving via the lung-to-ear pathway was computed as the sound impinging on the body wall (measured with the probe microphone) multiplied by the transmission gain of the lung-to-ear pathway (TG_L). Sound spectra were converted to complex numbers such that all addition was done vectorially and, thus, the resulting sum depended on both the amplitude and phase of each frequency. This sum of sound inputs was then multiplied by the transfer function of the ipsilateral tympanum ($H_I(\omega)$) to arrive at the predicted free-field transfer function. A range of weightings for TG_L (1 × to 6 ×) were explored in reconstructing free-field responses because local acoustic stimulation potentially underestimates the real magnitude of TG_L due to the smaller surface area of the body wall that is stimulated compared with free-field acoustic stimulation.

Bioacoustic analyses

We made acoustic recordings of green treefrogs in their natural habitat during active breeding choruses. Between 15 May and 3 July 2013, we recorded 457 advertisement calls from 23 males that were calling in ponds at the East Texas Conservation Center. These recordings (44.1 kHz, 16 bit) were made between 2300 and 0200 h using a Marantz PMD670 recorder (Marantz America, LLC., Mahwah, NJ) and handheld Sennheiser ME66/K6 microphone (Sennheiser USA, Old Lyme CT) held approximately 1 m from the focal animal. Male green treefrogs had a mean (±SD) SVL of 51.6 ± 3.9 mm and were recorded at a mean air temperature of 20.3 ± 3.0°C. Recordings of green frogs (*Lithobates clamitans*)[70] and bullfrogs (*Lithobates catesbeianus*)[71] were obtained during previous studies by one of the authors (MAB); the calls of the remaining eight frog species included in this study were obtained from the Macaulay Library at the Cornell Lab of Ornithology. For each species, we analyzed 6 to 23 calls per male (median = 20 calls per male) for each of 9 to 25 males (median = 20 males per species) by computing the power spectrum of each call using MATLAB's pwelch function (window size = 256, overlap = 50%). We determined the average call spectrum for a species by first averaging over the calls recorded from each individual and then over all individuals. Only recordings that were free from excessive background noise were included in these analyses.

Please cite this article in press as: Lee et al., Lung Mediated Auditory Contrast Enhancement Improves the Signal-to-Noise Ratio for Communication in Frogs, Current Biology (2021), https://doi.org/10.1016/j.cub.2021.01.048

Social network analysis of calling survey data

To generate frog species co-calling networks, we utilized a publicly available dataset from the North American Amphibian Monitoring Program (NAAMP).[53,54] Created as a citizen science collaboration between the United States Geological Survey (USGS) and a collection of state agencies, universities, and non-profit organizations, NAAMP was a long-term effort to monitor frog populations across 26 states in the eastern, central, and southern United States based on roadside calling surveys conducted by trained observers. Details about survey methods can be found elsewhere.[53,54] The NAAMP database consists of 319,765 observations of 57 identified species made during 21,934 roadside calling surveys conducted between 18 April 1994 and 9 August 2015. Fifteen of the 18 states encompassing the geographic range of green treefrogs, which are most abundant in the south-eastern United States, were included in the NAAMP dataset; therefore, coverage was high of geographic areas where green treefrogs were most likely to be heard calling. While the NAAMP dataset does not localize co-calling species precisely to the same body of water or close physical proximity, it represents the best (and only) measure of which other frog species might reasonably be expected to generate environmental noise for a green treefrog receiver in multi-species choruses across its geographic range on a continent-wide scale.

To create the co-calling network, we defined a node as a frog species and an edge as an event where both species were reported as calling during the same observation period (typically 3 min in duration) on the same date at the same survey stop at the same time of day. From networks containing only species co-occurring with green tree frogs (Figures 3, S4), we identified the top ten co-callers by selecting those with the ten highest edge weights. We analyzed networks with and without the inclusion of any species complexes that were not resolved to individual species in the NAAMP dataset (e.g., *Pseudacris feriarum/fouquettei* complex). When using green treefrogs as the focal species, inclusion or exclusion of species complexes did not alter the top ten co-calling species identified. To aid in visualization of the network for Figure 3, we took the square root of the raw edge weights and scaled this quantity by a factor of 15. All network analyses and images were generated in the *igraph* package in R (Version 3.3.2).[72]

Model of peripheral frequency selectivity

We modeled frequency selectivity in green treefrogs by creating a bank of hypothetical excitatory frequency tuning curves for 161 auditory nerve fibers. The shape of each modeled tuning curve, plotted as a thin line in Figure 4, was determined as a 4th order gammatone filter.[56,73,74] The best sensitivity of each modeled tuning curve was adjusted to match the best excitatory frequency and threshold for a given nerve fiber based on previously published results reported in Figure 1B of Ehret and Capranica.[51] That study reported data for 177 nerve fibers. We were able to extract data for 174 of these fibers from their published figures using DataThief III.[75] Following Ehret and Capranica,[51] we excluded 13 units with best excitatory frequencies between 1300 and 2800 Hz from consideration because these were observed to occur in only one frog and were not considered by those authors to be representative. The bandwidth of each modeled tuning curve was estimated using the best-fit regression line for Q_{10dB} as a function of threshold [computed based on data from Figure 2B in Ehret and Capranica[51]] to derive a predicted value of Q_{10dB} for each combination of best excitatory frequency and threshold. This estimate was used to compute the corresponding bandwidth 10 dB above threshold for each modeled tuning curve. (The joint relationship between best excitatory frequency, threshold, and bandwidth was not reported directly by Ehret and Capranica for[51] individual nerve fibers.)

QUANTIFICATION AND STATISTICAL ANALYSIS

Unless indicated otherwise, a significance criterion of $\alpha = 0.05$ was used. Two-tailed, one-sample t tests were used to test null hypotheses that there were no differences in tympanum vibration amplitude in response to free-field acoustic stimulation between the inflated and deflated states of lung inflation (n = 21). A two-tailed Pearson correlation was used to investigate the relationship between the peak frequency of the lungs in the inflated state and SVL (n = 10). We used a two-tailed, paired-sample t test of the null hypothesis that deflating the lungs would not change the magnitude of the peak frequency of the lung's resonance (n = 10). A two-tailed, paired-sample t test was used to directly compare the magnitudes of the resonance peak of the lungs in the inflated and reinflated states of inflation (n = 10). We also used two-tailed, one-sample t tests of the hypothesis that mean magnitudes of reduction in tympanum sensitivity were nonzero for three sound incidence angles (0°, −30°, and −60°) for each of five heterospecific species (15 comparisons total; n = 21 individuals for each comparison). All 15 comparisons remained significant after using the Holm-Šídák test to control for multiple comparisons; unadjusted p values are reported in Table S1.

Current Biology, Volume *31*

Supplemental Information

Lung Mediated Auditory Contrast Enhancement Improves the Signal-to-Noise Ratio for Communication in Frogs

Norman Lee, Jakob Christensen-Dalsgaard, Lauren A. White, Katrina M. Schrode, and Mark A. Bee

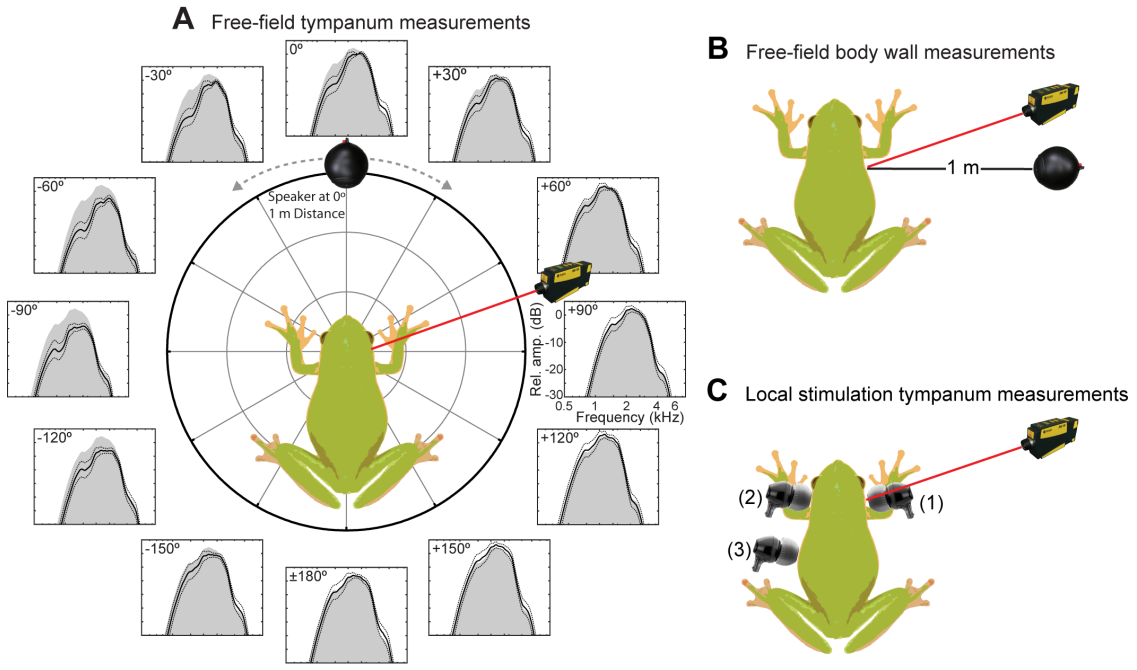

Figure S1. Laser vibrometry measurement of the vibration amplitudes of the right tympanum and right body wall overlying the lung in response to acoustic stimulation. Related to STAR Methods.

(A) The frequency spectrum of the vibration amplitude of the right tympanum was measured under free-field acoustic conditions in response to an FM sweep presented at each of 12 sound incidence angles (0° to ±180° in 30° steps) surrounding the animal from a speaker located 1 m away. These measurements were used to determine the impacts of the lungs on the tympanum's response under conditions of free-field acoustic stimulation. *Insets*: Spectra show the tympanum's mean (solid black line) ± 1 SD (dashed black lines) relative vibration amplitude as a function of frequency and sound incidence angle; the shaded gray area corresponds to the spectrum at +90° and is reproduced for comparison purposes at all other angles of sound incidence.

(B) The frequency spectrum of the vibration amplitude of the right body wall overlying the lung was measured under free-field acoustic conditions in response to an FM sweep presented from a speaker located 1 m away at an ipsilateral (+90°) angle of sound incidence. These measurements were used to determine the resonance frequency of the lungs under conditions of free-field acoustic stimulation.

(C) Local acoustic stimulation of the ipsilateral (to the laser) tympanum (1), the contralateral tympanum (2), and the contralateral body wall (3) was used to generate quantitative measures of the transmission gain of indirect sound input to the internal surface of the ipsilateral tympanum via the lungs and the contralateral tympanum.

(A-C) The laser used for measurements was always located to the frog's right side at an angle of +70° relative to the snout (at 0°).

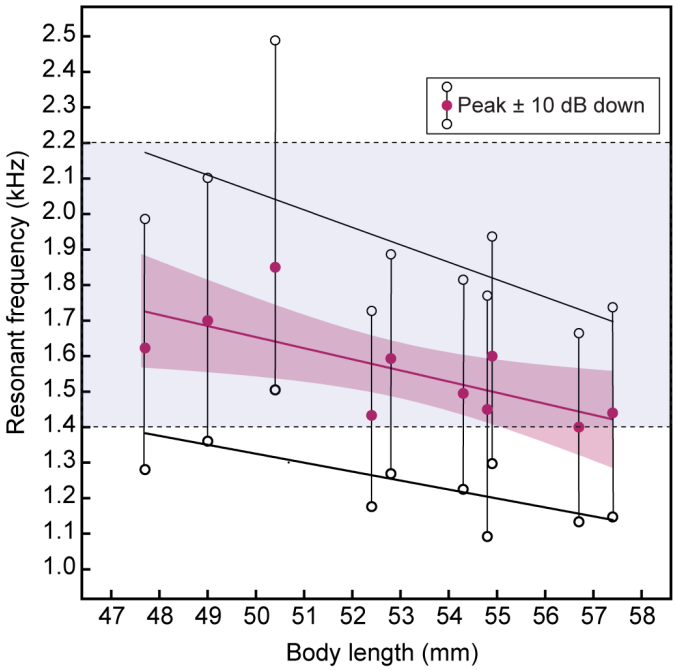

Figure S2. Frog lungs are size-dependent resonators. Related to Figure 2.
Under free-field acoustic stimulation by an FM sweep, the inflated lungs of green treefrogs exhibit a size-dependent resonance. There was a significant negative correlation between peak resonance frequency and body size, as expected if lung volume varies directly with body size (two-tailed Pearson $r = -0.705$, $R^2 = 0.498$, $p = 0.0228$). Filled circles depict, as a function of body length (snout-to-vent length), the mean peak resonance frequency of the body wall overlying the right lung in response to free-field acoustic stimulation by an FM sweep and measured using laser vibrometry (Figure S1B). Open circles connected to each peak frequency represent the ±10-dB down points on the resonance spectrum measured relative to the amplitude of the peak frequency. The colored line is the best-fit regression line (±95% CI) for the peak frequency; black lines depict best-fit lines for the upper or lower 10-dB down points. The shaded blue rectangle represents the frequency range of maximal attenuation of the green treefrog's tympanum vibration amplitude (1400 to 2200 Hz) as a result of lung inflation.

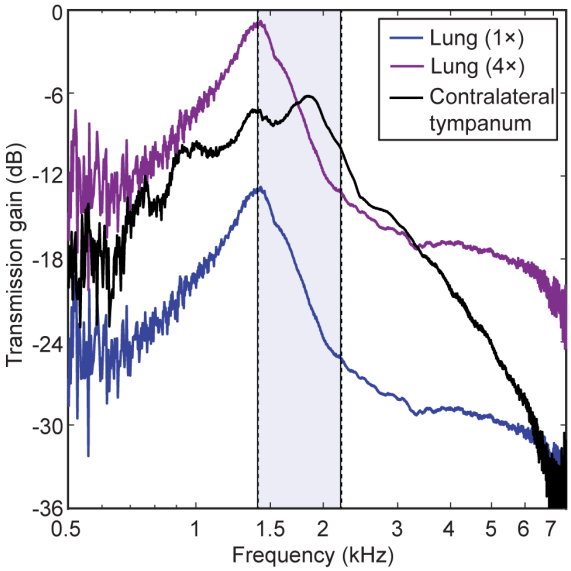

Figure S3. Transmission gain measurements reveal strong coupling between inflated lungs and the tympanum. Related to Figure 2.

Shown here are transmission gains of indirect sound input to the tympanum's internal surface from the lungs and contralateral tympanum relative to direct acoustic stimulation of the external surface and measured using local acoustic stimulation by an FM sweep (Figure S1C). The shaded blue rectangle represents the frequency range of maximal attenuation of the green treefrog's tympanum vibration amplitude (1400 to 2200 Hz) as a result of lung inflation. The transmission gains depicted here reflect how efficiently each indirect sound input is coupled to the tympanum's internal surface relative to sound arriving directly at its external surface. A transmission gain of 0 dB indicates sounds impinge on the internal and external surfaces with equal amplitudes and interact depending on their relative phases; negative values indicate sound reaches the internal surface of the tympanum at a relatively lower amplitude. The peak transmission gain of the lungs occurred at 1430 Hz. Unweighted (1×), the peak transmission gain of the lungs was -13 dB. A transmission gain weighting of 4× corresponds to a lung transmission gain amplitude that is 12 dB higher than the unweighted estimate. Hence, the peak transmission gain from the lungs is probably closer to -1 dB relative to the direct sound input to the tympanum's external surface. By comparison, the median peak transmission gain of input from the contralateral tympanum occurred at 1855 Hz and was -6 dB relative to direct stimulation of the tympanum's external surface. These measurements, therefore, indicate sound transmission to the internal surface of the tympanum through the lungs is likely quite substantial, exceeding by 5 dB input from the contralateral tympanum and, at the lung resonance frequency, being nearly equivalent to direct sound stimulation of the tympanum's external surface.

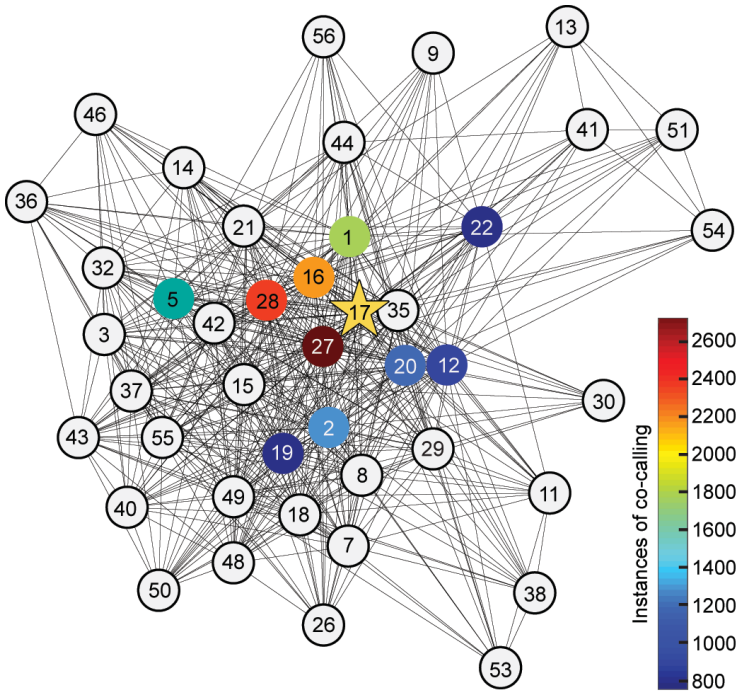

Figure S4. Social network analysis of data from the North American Amphibian Monitoring Program (NAAMP) identified 42 heterospecific, co-calling species. Related to Figure 3.

Using network analysis, we determined the incidence of "co-calling" between green treefrogs and other calling frog species in the NAAMP dataset. Green treefrogs were present on 9245 (2.9%) of the observations in the NAAMP dataset. Within these observations, a total of 42 heterospecific species co-called with green treefrogs. The top-10 co-callers are indicated by colored circles, with the number of observations of co-calling for each species (out of 19,809 total co-calling observations) depicted by the color map. The species identity for each numbered node is as follows: 1 *Acris crepitans*, 2 *Acris gryllus*, 3 *Anaxyrus americanus*, 5 *Anaxyrus fowleri*, 7 *Anaxyrus quercicus*, 8 *Anaxyrus terrestris*, 9 *Eleutherodactylus cystignathoides*, 11 *Eleutherodactylus planirostris*, 12 *Gastrophryne carolinensis*, 13 *Gastrophryne olivacea*, 14 *Hyla andersonii*, 15 *Hyla avivoca*, 16 *Hyla chrysoscelis*, 17 *Hyla cinerea*, 18 *Hyla femoralis*, 19 *Hyla gratiosa*, 20 *Hyla squirella*, 21 *Hyla versicolor*, 22 *Incilius nebulifer*, 26 *Lithobates capito*, 27 *Lithobates catesbeianus*, 28 *Lithobates clamitans*, 29 *Lithobates grylio*, 30 *Lithobates heckscheri*, 32 *Lithobates palustris*, 35 *Lithobates sphenocephalus*, 36 *Lithobates sylvaticus*, 37 *Lithobates virgatipes*, 38 *Osteopilus septentrionalis*, 40 *Pseudacris brimleyi*, 41 *Pseudacris clarkii*, 42 *Pseudacris crucifer*, 43 *Pseudacris feriarum*, 44 *Pseudacris fouquettei*, 46 *Pseudacris kalmi*, 48 *Pseudacris nigrita*, 49 *Pseudacris ocularis*, 50 *Pseudacris ornata*, 51 *Pseudacris streckeri*, 53 *Rhinella marina*, 54 *Scaphiopus couchii*, 55 *Scaphiopus holbrookii*, 56 *Scaphiopus hurterii*, 57 *Spea bombifrons*.

Species	Sound incidence	Attenuation (dB)	*t*	*p*	df
Lithobates clamitans	0°	-4.4 ± 1.9	-4.38	< 0.001	20
	-30°	-4.5 ± 2.2	-3.98	0.001	20
	-60°	-5.4 ± 2.2	-4.89	< 0.001	20
Lithobates catesbeianus	0°	-4.0 ± 1.9	-4.06	0.001	20
	-30°	-4.1 ± 2.2	-3.70	0.001	20
	-60°	-5.0 ± 2.1	-4.76	< 0.001	20
Incilius nebulifer	0°	-3.9 ± 2.0	-3.83	0.001	20
	-30°	-4.5 ± 2.5	-3.43	0.003	20
	-60°	-3.8 ± 2.5	-3.01	0.007	20
Anaxyrus fowleri	0°	-3.6 ± 1.9	-3.63	0.002	20
	-30°	-3.8 ± 2.2	-3.39	0.003	20
	-60°	-4.6 ± 2.0	-4.43	< 0.001	20
Hyla gratiosa	0°	-4.4 ± 1.9	-4.38	< 0.001	20
	-30°	-4.5 ± 2.2	-3.98	0.001	20
	-60°	-5.4 ± 2.2	-4.89	< 0.001	20

Table S1. Lung-mediated attenuation of spectral peaks in heterospecific calls. Related to Figure 3.

Mean (± 95% CI) attenuation as a result of lung inflation of the amplitude of the spectral component in or closest to the range of 1400 to 2200 Hz in five heterospecific species' advertisement calls in the frontal field (0°) or in the contralateral field (-30° and -60°) relative to the position of the measurement laser. The species included here represent the five species from among the top-10 co-callers for which the benefit to green treefrogs of lung-mediated attenuation of tympanum vibrations would be most pronounced. These co-callers produce advertisement calls with substantial acoustic energy in the frequency range of 1400 to 2200 Hz and frequently co-call with green treefrogs according to the North American Amphibian Monitoring Program dataset (Figures 3 & S4). Statistical results are from two-tailed, one-sample t-tests (n = 21 individuals).